Linearization and Modal Analysis of Flexible Rocking Structures

S. Acikgoz, M. J. DeJong

University of Cambridge, Cambridge, United Kingdom

2013 NZSEE Conference

ABSTRACT: Recent years have seen a growing interest in utilizing rocking mechanisms for the earthquake resistant design of structures. In particular, base rocking mechanisms have been implemented in several building and bridge systems, and their effectiveness in eliminating residual damage has been demonstrated in experimental and computational studies. To improve the current understanding of how rocking structures respond to dynamic excitation, and to generalize this response as much as possible, this paper focuses on fundamental dynamics. A generic analytical model of an elastic multiple degree of freedom (MDOF) structure, allowed to freely rock at its base on a rigid rocking interface, is considered. To address the dynamics of controlled rocking structures, a central elastic post-tensioned tendon and a viscous damper, which provide additional self-centering force and energy dissipation, are also incorporated. The equations of motion describing the rocking motion are derived for large rotations using a Lagrangian formulation. These equations are then linearized about the initial (at-rest) position. The subsequent eigenvalue analysis of the linearized system provides valuable information on how rocking modifies elastic action, and vice versa. The trends revealed by the analysis indicate that the rocking action primarily influences the first few modes of the structure.

1 INTRODUCTION

Modal analysis is an essential tool used in structural analysis to identify and reconstruct salient characteristics of response. For structures with nonlinear stiffness, non-classical damping and non-smooth discontinuities, modal analysis is often challenging to perform and the physical interpretation of the results may be difficult (Worden and Tomlinson 2001). In some cases, the problem can be linearized and the resulting formulation can be used to evaluate the fundamental dynamic characteristics of the system (Shaw and Pierre 1993; Makris and Palmeri 2008). Adopting this approach, this paper considers modal analysis of a MDOF flexible structure rocking on rigid ground. Contrasting the eigenvectors of the system before and during rocking motion provides valuable information on how rocking affects the elastic response, and vice versa. A brief discussion outlines how the results obtained from this modal analysis may be useful in formulating a simplified approach to analysis and design of rocking structures.

2 DERIVATION AND LINEARIZATION OF STRUCTURAL MODEL

2.1 The structural model

The structural model utilized in this study is shown in Figure 1. The superstructure is a generic elastic MDOF system which has n nodes, with both a lumped mass and a mass moment of inertia (associated to rigid body rotation of the node about its center of gravity). Each lumped mass m_i and rotational inertia J_i is located at horizontal distance B, height H_i and radius R_i relative to the edge of the rigid foundation beam. Masses are connected with axially rigid rods which allow translation (denoted by u_i in Fig 1) at each node. The model can be generalized to include rotational degrees of freedom at its nodes, however, only translation is considered in this study.

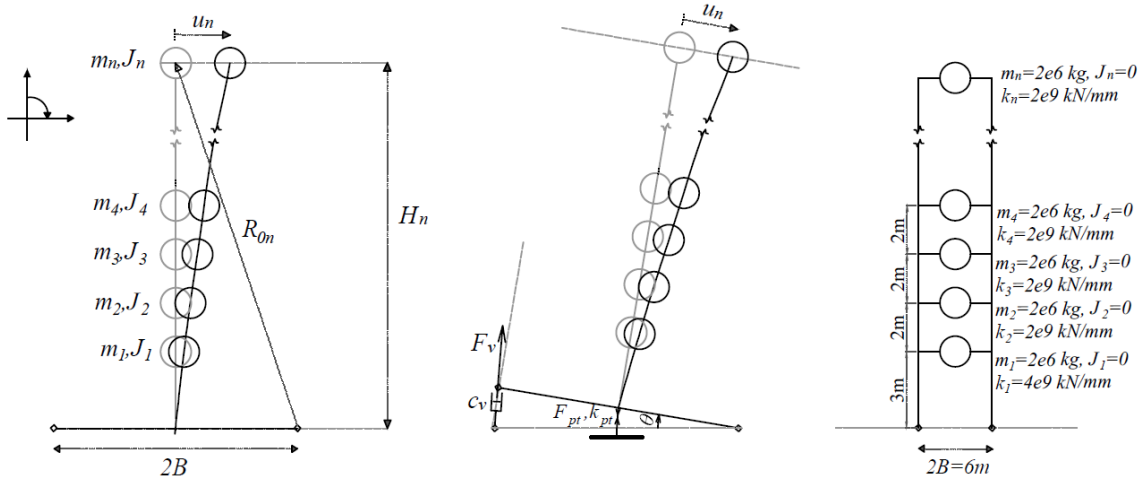

Figure 1 – Schematic of a MDOF elastic lumped mass structural model (left) during full contact phase and (middle) during rocking phase and (right) the idealized shear frame considered in this study

The structure is assumed to respond in two different phases to a given ground acceleration with horizontal and vertical components (represented by $\ddot{u}_g$ and $\ddot{v}_g$). For quiescent initial conditions, the initial response is elastic and the structure remains in full contact with the rigid ground (see Fig 1(left)). Once the conditions of uplift are met, the structure starts to rock about either of the pivot points, located under the edges of the rigid foundation beam (see Fig 1(middle)). Sliding at these pivot points is prevented and the rocking action is described by the angle θ between the foundation beam and the ground. For the freely rocking model (no tendon or dissipater), the self-centring force is due to the gravitational acceleration g. In the controlled rocking model, an elastic central tendon with stiffness k_{pt} and post-tension force F_{pt} provides an additional self-centring force, while an angular viscous damper located at each edge of the foundation beam, with damping coefficient c_v, dissipates additional energy.

2.2 **Nonlinear EoM**

Initially, the response to ground excitation is linear, and the structure remains in the full contact phase. Using the generalized coordinates u_i, for i = 1,..,n, the following equation of motion (EoM) describes the response:

$$[M]\ddot{\underline{u}} + [C]\dot{\underline{u}} + [K]\underline{u} = -[M]\underline{1}\,\ddot{u}_g \tag{1}$$

where the vectors $\underline{u}$, $\dot{\underline{u}}$ and $\ddot{\underline{u}}$ describe the nodal displacement, velocity and acceleration in the direction parallel to the rigid foundation beam. The diagonal mass matrix [M], the classical damping matrix [C] and the stiffness matrix [K] are conventionally defined.

Once the structure starts to rock, the EoM describing force equilibrium in the direction of the generalized coordinates u_i becomes nonlinear. Evaluating the Lagrangian for these coordinates yield:

$$[M]\ddot{\underline{u}} + [M]\underline{H}\ddot{\theta} + [M](\pm B\,\underline{1} - \underline{u})\dot{\theta}^2 + [C]\dot{\underline{u}} + [K]\underline{u} = -[M]\underline{1}\,\ddot{u}_g \cos\theta + [M]\underline{1}(\ddot{v}_g + g)\sin\theta \tag{2}$$

where the vector $\underline{H} = [H_1, H_2, ..., H_n]^T$ describes the height of each lumped mass before the initiation of rocking motion. Note that the upper sign denotes rocking about right pivot point and the lower sign denotes rocking about left pivot point. A similar notation will be used in the following equations.

An additional EoM is required to describe the moment equilibrium about the pivot point. Evaluating the Lagrangian for the generalized coordinate θ, this equation can be obtained as:

$$\begin{aligned}&\left(\underline{J}^T\underline{1}+\underline{R}^T[M]\underline{R}+\underline{u}^T[M]\underline{u}\mp 2B\underline{1}^T[M]\underline{u}\right)\ddot{\theta}+\underline{H}^T[M]\ddot{\underline{u}}\\&\mp 2\dot{u}^T[M](B\underline{1}\mp\underline{u})\dot{\theta}+2c_vB^2(1+\cos\theta)\dot{\theta}\pm F_{pt}B\cos(\theta/2)+k_{pt}B^2\sin\theta=\\&-\ddot{u}_g\left(\underline{H}^T[M]\underline{1}\cos\theta\pm\underline{1}^T[M](B\underline{1}\mp\underline{u})\sin\theta\right)-(\ddot{v}_g+g)\left(-\underline{H}^T[M]\underline{1}\sin\theta\pm\underline{1}^T[M](B\underline{1}\mp\underline{u})\cos\theta\right)\end{aligned}\tag{3}$$

where $\underline{R}$ represents the distance from each lumped mass to the pivot point before the initiation of rocking, and $\underline{J}$ represents the mass moment of inertia lumped at the centre of each node respectively. While equations to describe the dynamics of similar MDOF rocking systems have been proposed, nonlinearities associated with large rotations were previously ignored and approximate EoM centred around the at rest position were formulated (Psycharis 1983; Yim and Chopra 1985).

The effect of geometric nonlinearity can be observed from the right hand side of Equation 3. Depending on the rocking amplitude, the amount of self-centring force due to gravity and the relative effect of horizontal and vertical components of ground motion vary. The effective rotational inertia, the term in the first parenthesis of Equation 3, is dependent on the elastic deformation of the mass. The Coriolis and centrifugal acceleration terms observed in Equations 2-3 indicate the expected coupling due to the rotating reference frame. Additionally, nonlinear terms due to post-tensioned tendon and external damper can be identified in Equation 3 and these terms agree with previous investigations (Dimitrakopoulos and DeJong, 2012).

2.3 **Linearization of nonlinear EoM**

The geometric nonlinearity associated with rocking motion has been discussed in earlier studies on rigid rocking structures, wherein the EoMs were linearized about the unstable equilibrium point to simplify the overturning problem (Housner 1964). While this approach does not eliminate the nonlinearity arising from non-smooth transition between rocking cycles, it reduces the governing EoM into a piecewise linear formulation which may provide accurate approximations around the unstable equilibrium point (Allen and Duan 1995; Palmeri and Makris 2008). A similar linearization approach, outlined by Palmeri and Makris (2008), is adopted here. This investigation is primarily interested in the response of large structures which are typically limited to small rocking responses (Acikgoz and DeJong 2013). Therefore, Equations 2-3 are linearized about the initial position where $[u_1,u_2,...,u_N,\theta]=[0,0,...,0,0]$. Linearizing Equation 2 yields:

$$[M]\ddot{\underline{u}}+[M]\underline{H}\ddot{\theta}+[C]\dot{\underline{u}}+[K]\underline{u}=-[M]\underline{1}\ddot{u}_g+[M]\underline{1}(g)\theta\tag{4}$$

Similarly, linearizing Equation 3 yields:

$$\begin{aligned}&\left(\underline{J}^T\underline{1}+\underline{R}^T[M]\underline{R}\right)\ddot{\theta}+\underline{H}^T[M]\ddot{\underline{u}}+4c_vB^2\dot{\theta}\pm F_{pt}B+k_{pt}B^2\theta=\\&-\ddot{u}_g\left(\underline{H}^T[M]\underline{1}\right)\mp(\ddot{v}_g+g)\left(B\underline{1}^T[M]\underline{1}\right)+g\left(\underline{H}^T[M]\underline{1}\,\theta+\underline{u}^T[M]\underline{1}\right)\end{aligned}\tag{5}$$

After linearization, the equations have become 2nd order coupled linear differential equations and are fundamentally different from previously published equations which have ignored the negative stiffness during the rocking phase (Meek 1978; Yim and Chopra 1985). However, the linearized equations are similar to the equations derived by Psycharis (1983). As noted by Palmeri and Makris (2008), the linearization procedure is analogous to a first order approximation of a series around a point; the high order nonlinear terms arising from change in position of the structure have vanished in the linearized formulation. In fact, these equations can also be derived assuming an inertial reference frame.

It is possible to express Equations 4 and 5 as a single system of equations in matrix form where $[M_L],[C_L],[K_L]$ and $[F_L]$ represent the linearized system mass, damping, stiffness and forcing matrices, and can be directly derived from Equations 4 and 5. System mass, stiffness and damping matrices are symmetric although they are not diagonal or positive definite. The time dependent system variable $x=[u_1,u_2,...,u_n,\theta]^T$ encompasses all the variables in the system:

$$[M_L]\ddot{\underline{x}}+[C_L]\dot{\underline{x}}+[K_L]\underline{x}=[F_L]\tag{6}$$

3 MODAL ANALYSIS

3.1 State-Space Formulation

To perform modal analysis on the linearized system, the system velocities need to be expressed as separate dependent variables. Using the procedure of separation of variables, Equation 6 can be expressed in state-space formulation. Setting $[F_L] = 0$ the homogenous ordinary differential equation in state-space form is given by:

$$\frac{d}{dt}\begin{pmatrix} x \\ \dot{x} \end{pmatrix} = \begin{bmatrix} 0[I] & [I] \\ -[M_L]^{-1}[K_L] & -[M_L]^{-1}[C_L] \end{bmatrix} \begin{bmatrix} x \\ \dot{x} \end{bmatrix} \tag{7}$$

where $[I]$ is the identity matrix which has the same dimensions as $[M_L]$. After assuming that the system has solutions of the form $x_j = \underline{\phi_j} e^{\lambda_j t}$, where λ_j and $\underline{\phi_j}$ are the system's j^{th} eigenvalue and eigenvector, substitution of this relation into Equation 7 leads to a typical eigenvalue problem. Using this formulation allows uncoupling of the vibration modes of structures where damping is non-classical and normal decomposition methods are not applicable (Foss, 1958).

The linearized equations of motion are coupled and this results in complicated expressions. In this study, the eigenvalue problem will instead be solved numerically for an example structure, and the results will then be generalized.

3.2 Numerical Example

The 7-story shear frame shown in Figure 1(right) is considered in this study. The choice of the specific shear frame has limited significance in this work as the results are meant to exemplify general trends. In order to gain a physical understanding of the problem, an undamped superstructure allowed to rock freely will be initially examined. This particular case yields eigenvalues and eigenvectors which have either real or imaginary components and therefore the eigenvectors have clear physical meaning. Later, a classically damped superstructure with post-tensioning and viscous angular damping is considered, and the effect of each element on the eigenvalues of the system is briefly discussed.

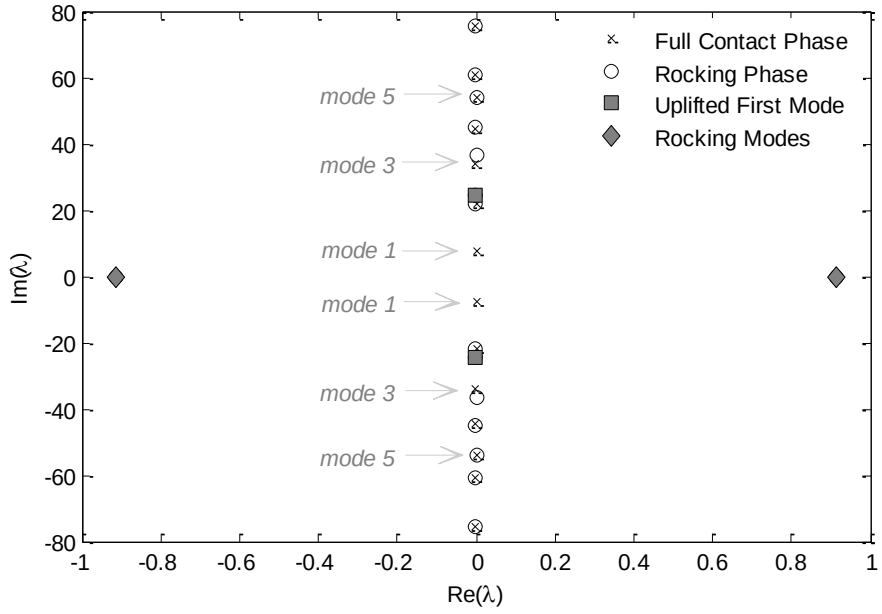

Figure 2 - Comparison of the eigenvalues of the undamped shear frame during full contact and rocking phases. The eigenvalues of the first, third and fifth modes during full contact stage are highlighted with arrows while the uplifted first mode and rocking mode are highlighted with markers.

3.2.1 *Orthogonal Modes of the Undamped Superstructure*

The eigenvalues of the system in the full contact stage and rocking stage are computed numerically and are shown in the complex plane in Figure 2. All eigenvalues have a complex conjugate, therefore eigenvalues are symmetric about the origin. All of the eigenvalues of the full contact stage (shown with marker x) lie on the imaginary axis. This is expected as the superstructure is undamped; during full contact, each mode is a simple harmonic with a discrete frequency.

The eigenvalues of the rocking phase (shown with marker ∘) are slightly different. First, for the normal modes of motion which lie on the imaginary axis, there is good agreement between the eigenvalues of the full contact and rocking phases. The most significant exception is the first mode, which lies close to the origin for the full contact phase, due to its low frequency. However, once rocking initiates, a decrease is observed in the effective modal mass participating in this mode, resulting in an uplifted 1st mode with a much higher frequency (3.2 times higher, shown with the grey filled marker ■) . Despite its increased frequency, this mode will still be referred to as the uplifted first mode due to its mode shape which resembles its full contact counterpart (see Fig 3). The third mode eigenvalues are also notably different, although the difference is less drastic than that of the first mode.

An additional eigenvalue couple (highlighted with grey filled markers ♦) lying on the real axis, is observed during the rocking phase. These eigenvalues are real valued; a positive real eigenvalue implies an unstable solution which keeps increasing infinitely and a negative real eigenvalue implies a stable solution which decays asymptotically to zero. The presence of these real-valued eigenvalues implies a hyperbolic solution. These are readily identified as rocking modes, similar hyperbolic solutions have been obtained for the linearized EoM of the rigid rocking block (Housner 1963).

The eigenvectors associated to the eigenvalues shown in Figure 2 are presented in Figure 3 for the full contact phase and the rocking phase. The eigenvectors are scaled to a Euclidean norm of unity. Initially, the rotation component of the eigenvectors of the rocking phase is removed, and only the translational eigenvector ordinate corresponding to each node is plotted (i.e. j^{th} eigenvector $\underline{\phi_j}$ is

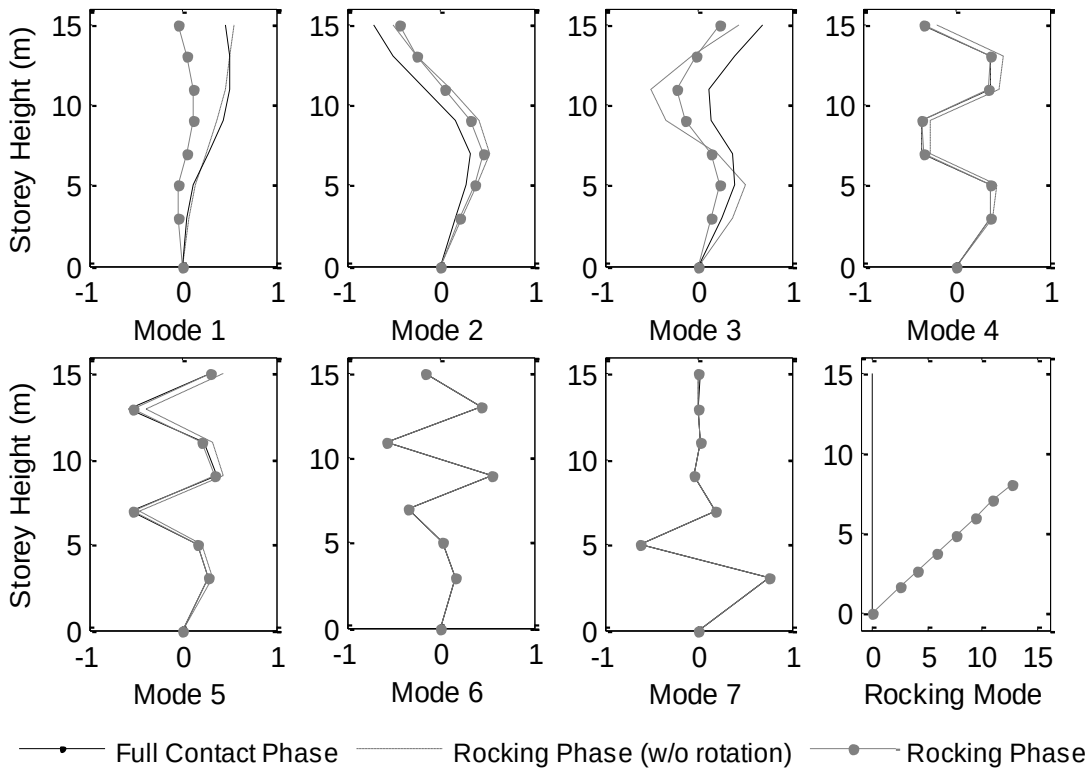

Figure 3 – Comparison of the eigenvectors of the undamped shear frame during full contact and rocking phases

plotted against $\underline{H}$). This representation allows direct comparison of the translational component of motion during full contact (dashed line) and rocking phases (solid black line). To show the magnitude associated with the rotation component of each mode, the complete eigenvectors of the rocking phase (including the rotational component) are also shown (solid grey line with marker •). Note that after including the rotational component of the eigenvectors, the vertical and horizontal axes no longer represent the storey height and eigenvector ordinates precisely.

Figure 3 shows how the eigenvectors change once rocking is initiated (observe the changes from dashed to solid black lines) and how rocking action is coupled with the elastic action (observe the changes from solid black to grey lines with markers). Although quite small in some cases, all harmonic modes feature a rocking component that counteracts the elastic action. The rocking component is particularly strong for the first, second and third mode eigenvectors. It is no surprise that these are also the modes where the largest discrepancy is observed between the full contact and rocking eigenvalues. This suggests stronger coupling between elasticity and rocking in these modes. In particular, for the 3rd mode, this coupling seems to have altered the mode shape significantly. This coupling might be a result of the major contribution of these modes to the base overturning moment. Finally, note that the rocking mode, shown in the final subfigure (bottom right), features very small elastic action and quite large rotation action. This implies that the rocking mode describes the rigid body rotation of the structure as a whole.

Earlier, by classical mode decomposition and a subsequent Laplace transform of the governing linear EoM, Psycharis (1983) had demonstrated the presence of hyperbolic and harmonic solutions of the MDOF rocking system. Qualitatively, Psycharis (1983) observed the strong interaction between the first mode and the rocking mode, and suggested that higher modes are relatively unaffected by the rocking motion. The results presented above generally agree with these important trends. However, the eigenvectors of the 2nd and 3rd modes clearly show that classical mode decomposition is not valid for an uplifting structure, although it might be a useful approximation. Furthermore, the demonstrated eigenvalues and eigenvectors during full contact and rocking phases quantify the interaction of elasticity and rocking and allow the reconstruction of response from modal constituents.

3.2.2 *Damped superstructure with free and controlled rocking action*

Rayleigh damping was assigned to the superstructure where a fraction of critical damping of 5% was specified for the first and third modes of the structure. Despite the use of proportional

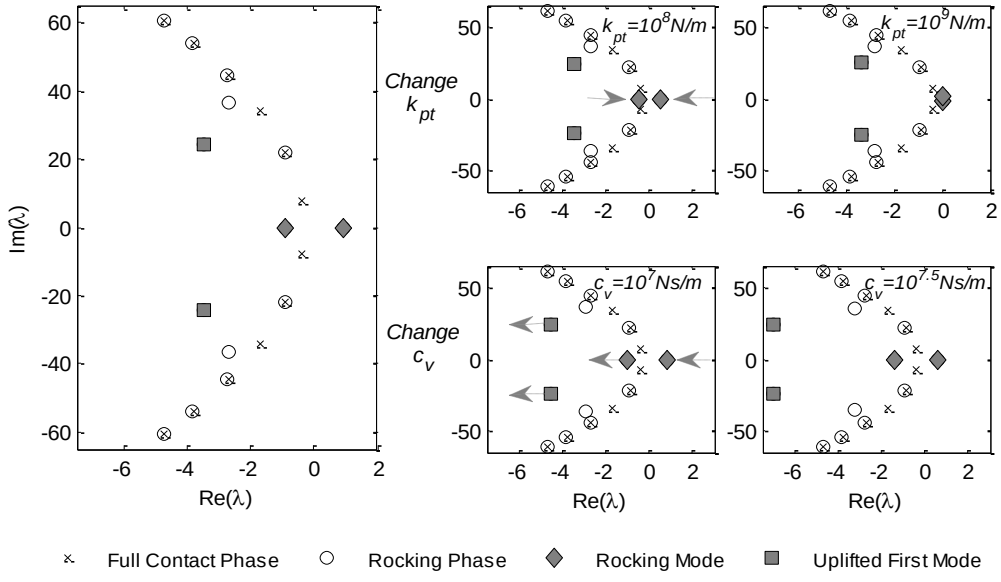

Figure 4 –The eigenvalues of a classically damped shear frame (left) allowed to rock freely, (top right) with a posttensioning elastic tendon and (bottom right) with an external viscous dissipater.

superstructure damping, the system damping matrix $[C_L]$ is non-classical due to the presence of rocking action (Caughey and O'Kelly, 1965). In Figure 4 (left), the eigenvalues for this system are shown in the complex plane. Due to the introduction of damping, the eigenvalues of the full contact phase have a negative real component, which suggests decaying motion, alongside an imaginary component, which implies vibration. Just as in the undamped case, there is good agreement between the majority of the eigenvalues of full contact and rocking phases. However, as with the undamped case, the frequency of first mode (shown with the grey filled marker ■) drastically increases once the rocking phase is initiated. For the damped superstructure, this increase is accompanied by an increase in the effective damping factor, resulting in a high frequency and highly damped first mode response. A similar phenomenon was observed for a 2DOF rocking system previously investigated by the authors (Acikgoz and DeJong 2012), and in experimental investigations (Evison 1977, Ma 2010). It should be noted that the real valued symmetric eigenvalues pertaining to the rocking mode are also observed in this figure and are of the same magnitude as in the undamped case. This is expected as the eigenvalue of the rocking mode relates closely to the frequency parameter discussed by Housner (1963), which is only a function of the scale and rotational inertia of the structure. The rocking mode eigenvalue is therefore insensitive to changes in superstructure stiffness and damping.

The effects of adding a post-tensioned tendon or an external viscous damper were also investigated. Eigenvalue results are presented in Figure 4, considering the same damped superstructure. In the top right of Figure 4, the rocking phase eigenvalues for different levels of tendon stiffness are presented. Similarly, in the bottom right of Figure 4, the rocking phase eigenvalues for different levels of viscous angular damping are presented.

The effect of increasing the tendon stiffness has a significant effect on the rocking mode eigenvalue and a small effect on the harmonic mode eigenvalues**.** An increase in tendon stiffness increases the self-centring force. This has a similar effect as an increase in the scale of the structure, which decreases the frequency parameter (Acikgoz and DeJong, 2013) and hence causes the real-valued rocking eigenvalues to approach the origin. In the extreme, when the stiffness provided by the tendon is so high that it provides the bulk of the self-centring stiffness, the rocking mode eigenvalue also becomes harmonic and lies on the imaginary axis. On the other hand, external viscous damping affects both the rocking and first modes significantly, while its effect on higher modes is relatively small. Increasing external viscous damping causes an increase in the magnitude of the eigenvalue of the stable component of the rocking mode, while decreasing the unstable component (similar results were obtained for the retrofitted rigid block in Dimitrakopoulos and DeJong 2012). Furthermore, due to coupling between rocking and elastic action, an increase in the viscous damping results in a significant increase in the damping component of the harmonic first mode.

4 CONCLUSIONS

This paper aims to better understand the complicated dynamics of flexible rocking structures through the use of modal analysis. After the derivation and linearization of novel EoMs describing the nonlinear response of a MDOF structure rocking on rigid ground, modal analysis was performed numerically for an idealized 7-story shear frame building allowed to uplift. All vibration modes were found to interact with the rocking motion, and this interaction was quantified. Rocking was found to completely alter the first mode; its eigenfrequency and modal damping were found to increase significantly. In general, higher mode eigenvalues did not change drastically upon the initiation of rocking, although the eigenvectors for the 2nd and 3rd mode suggest distinct behaviour due to rocking action. These trends were observed for both free and controlled rocking systems. Furthermore, it is shown that the response of the rocking mode is strongly dependent on the available self-centring force and is not significantly affected by superstructure lateral stiffness and damping.

The important trends observed in this study generally agree with earlier analytical investigations (Psycharis, 1983) and more recent computational and experimental studies (Wiebe et al 2012; Widodo 1995). The analytical approach to modal decomposition revealed the presence of orthogonal modes, which quantify the interaction of vibration and rocking, allowing the reconstruction of a more accurate linearized response. However, it is still necessary to quantify the importance of nonlinearities on the

global response, which can be achieved using the new nonlinear formulations presented in this paper. Particularly, it is important to quantify the nonlinearity due to impact. Non-smooth discontinuity of the equations of motion at impact may excite different vibration modes, which in turn would influence the overall rocking and elastic deformation behaviour.

REFERENCES

Acikgoz, S., & DeJong, M. J. 2012. The interaction of elasticity and rocking in flexible structures allowed to uplift. *Earthquake Engineering & Structural Dynamics*, *41*:2177–2194.

Acikgoz, S., & DeJong, M. J. 2013. The response of large rocking structures to earthquakes. *Manuscript submitted for publication*.

Allen, R. H., & Duan, X. 1995. Effects of Linearizing on Rocking-Block Toppling. *Journal of Structural Engineering*, *121:*1146–1149.

Caughey T. K., & O'Kelly M. E. J. 1965. Classical normal modes in damped linear dynamic systems. *Journal of Applied Mechanics*, *32*:583–588.

Dimitrakopoulos, E., & DeJong, M.J. 2012. Overturning of Retrofitted Rocking Structures under Pulse-Type Excitations. *Journal of Engineering Mechanics, 138:* 963–972.

Evison, R. J. 1977. *Rocking Foundations.* M.E. Thesis. University of Canterbury: NZ.

Foss, K. A. 1958. Co-ordinates Which Uncouple the Equations of Motion of Damped Linear Dynamic Systems. *Journal of Applied Mechanics*, *25*:361–364

Housner, G. W. 1963. Behaviour of Inverted Pendulum Structures During Earthquakes. *Bulletin of the Seismological Society of America*, *53*: 403–417.

Ma, Q.T. 2010. *Mechanics of Rocking Structures Subjected to Ground Motion*. Ph.D. Thesis. University of Auckland: NZ.

Meek, J. 1978. Dynamic response of tipping core buildings. *Earthquake Engineering & Structural Dynamics*, *6*:437–454.

Palmeri, A., & Makris, N. 2008. Linearization and first-order expansion of the rocking motion of rigid blocks stepping on viscoelastic foundation. *Earthquake Engineering & Structural Dynamics*, *37*: 1065–1080.

Psycharis, I. N. 1983. Dynamics of flexible systems with partial lift-off. *Earthquake Engineering & Structural Dynamics*, *11*: 501–521..

Shaw, S., & Pierre, C. 1993. Normal modes for non-linear vibratory systems. *Journal of Sound and Vibration*, *164*: 85–124.

Widodo. 1995. *Rocking of Multistorey Buildings*. Ph.D. Thesis. University of Canterbury: NZ.

Wiebe, L., Christopoulos, C., Tremblay, R., & Leclerc, M. 2012. Mechanisms to limit higher mode effects in a controlled rocking steel frame . 1 : Concept , modelling , and low-amplitude shake table testing. doi:10.1002/eqe.2259

Worden, K., & Tomlinson, G. R. 2001. Nonlinearity in experimental modal analysis. *Proceedings of the Royal Society A*, *359:* 113–130.

Yim, C. S., & Chopra, A. K. 1985. Simplified earthquake analysis of multistory structures with foundation uplift. *Journal of Structural Engineering*, *111:* 2708.